JOM, Vol. 66, No. 4, 2014
DOI: 10.1007/s11837-014-0945-8


# Plasma Synthesis of Nitrogen Clusters on Carbon Nanotube Sheets

EL MOSTAFA BENCHAFIA,[1] CHI YU,[1] MAREK SOSNOWSKI,[2] N.M. RAVINDRA,[1] and ZAFAR IQBAL[3,4]

1.—Interdisciplinary Program in Materials Science and Engineering and Department of Physics, New Jersey Institute of Technology, Newark, NJ 07102, USA. 2.—Electrical and Computer Engineering Department, New Jersey Institute of Technology, Newark, NJ 07102, USA. 3.—Department of Chemistry and Environmental Science, New Jersey Institute of Technology, Newark, NJ 07102, USA. 4.—e-mail: zafar.iqbal@njit.edu

The radio frequency plasma synthesis of nitrogen clusters stabilized on carbon nanotube sheets has been demonstrated under various conditions. Characterization of the samples produced has been carried out using micro-Raman and attenuated total reflectance-Fourier transform infrared spectroscopy. Initial investigations of the sample morphologies and compositions have also been performed using scanning electron microscopy combined with energy-dispersive x-ray analysis and transmission electron microscopy. The spectroscopic results, together with density functional theory calculations, suggest that a linear chain nitrogen cluster is formed under the plasma conditions employed and is stabilized most likely inside the walls of the carbon nanotubes that are used as substrates during the synthesis.

## INTRODUCTION

The explosive transformations of single- and/or double-bonded all-nitrogen compounds provide a promising high-energy release for energetic applications. Estimates suggest a tenfold improvement in detonation pressure[1] over the widely used energetic material HMX ($C_4H_8N_8O_8$). The potential application of an all-nitrogen compound as a high-energy density material drew so much interest that extensive theoretical studies have been conducted to give insights about the possible structural and electronic configurations that the polymeric nitrogen (referred to as PN throughout this article) can adopt. The azide anion $N_3^-$ has been known for more than a century as salt like sodium azide and can be considered to be an ionic oligomeric form of PN with two of its resonance structures shown below:

$$[\langle N = N = N\rangle]^- \equiv \left[\left|\underline{\bar{N}} - N \equiv N\right|\right]^-, \qquad (1)$$

where a triple bond occurs in one of the resonance structures, giving this compound the energy storage capability to transform into molecular nitrogen under specific conditions. In 1999, a breakthrough attempt to synthesize a higher oligomer of PN was the successful synthesis of the $N_5^+AsF_6^-$ compound,[2] where the pentanitrogen cation $N_5^+$ constituted a possible backbone for polymerization toward an all-nitrogen compound with 10 or more nitrogen atoms. In 2004, a high-temperature/high-pressure approach, using a diamond anvil cell under 110 GPa and 2000 K, was performed by Eremets et al.[3] to successfully produce the predicted cubic-gauche (Fig. 1) structure.[4] However, no attempts have been made to obtain this all nitrogen single-bonded structure under ambient conditions. Earlier work, also by Eremets et al.[5] using high-pressure/high-temperature conditions, indicated the formation of a semiconducting amorphous phase. Another structure, referred to as the chaired web (cw), which has an insulating rhombohedral structure (Fig. 2), was predicted by Zahariev et al.[6] to be thermodynamically more favored than the cubic-gauche phase at zero pressure by 20 meV, but it has not yet been experimentally observed.

Possible routes to a potentially stable $N_8$ neutral cluster from the $N_3^-$ and $N_5^+$ ion pair was theoretically explored by Fau and Bartlett.[7] A dissociation barrier that is at least 10 kcal/mol lower than needed was calculated. Therefore, the ion pair can be only stabilized in a solid with large lattice energy. In


(Published online April 1, 2014)

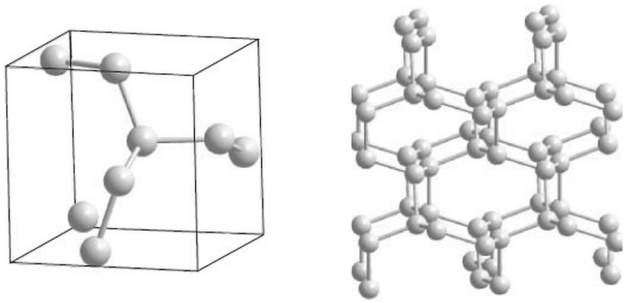

Fig. 1. Polymeric cubic gauche structure (cg-PN) structure, primitive cell (left) and an extended structure (right).[3]

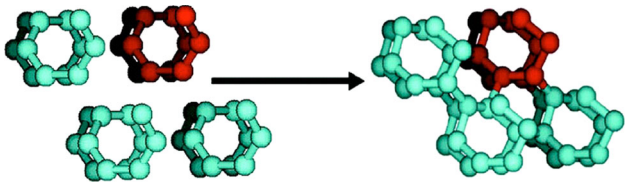

Fig. 2. Schematic of an optimally arranged set of sixfold helices (left) forming the single-bonded chaired web structure of PN.[6]

a recent study,[8] an interesting molecular crystal containing uncharged $N_8$ linear chain molecular clusters was predicted to be metastable at ambient pressures with energies below that of the cubic gauche phase (Figs. 3 and 4).

$N_8$ Chains and $N_{24}$ encapsulated inside carbon nanotubes, shown in Fig. 5, was proposed by Abou-Rachid et al.[9] Carbon nanotubes are demonstrated to be ideal hosts to confine the highly metastable PN by providing stability through the hybridization that takes place between the nanotubes and PN conduction bands. Confining PN under ambient conditions is an interesting approach. The relative thermodynamic instability of polymeric nitrogen compounds can be overcome by providing kinetic stability through hybridization by a charge-transfer mechanism and thus the high lattice energy requirement to gain stability and avoid the explosive conversion to molecular $N_2$.

In the current work, the method of plasma-enhanced chemical-vapor deposition has been adopted using nitrogen or ammonia combined with either argon or hydrogen as feeding gases as a novel approach to synthesize PN under low-pressure conditions and plasma temperatures between 100°C and 400°C. In a variation of this approach, sodium azide was used as the nitrogen precursor by dipping the carbon nanotube sheets or nanopaper substrates in aqueous solutions of sodium azide and then carrying out the plasma reaction under nitrogen-argon or nitrogen-hydrogen feeding gases. This article will be focused on the samples produced using sodium azide as the precursor together with a comparison in some instances of samples produced using nitrogen mixed with argon as the carrier gas.

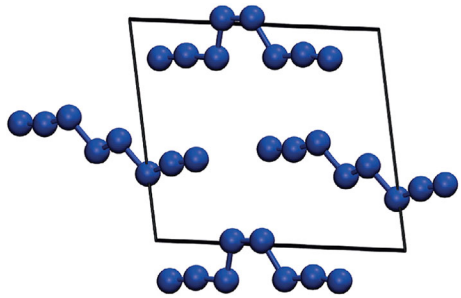

Fig. 3. Unit cell of predicted $N_8$ solid.[8] Top and bottom layer conformational isomer of $N_8$ in the unit cell is referred to as EZE and the middle layer as EEE.

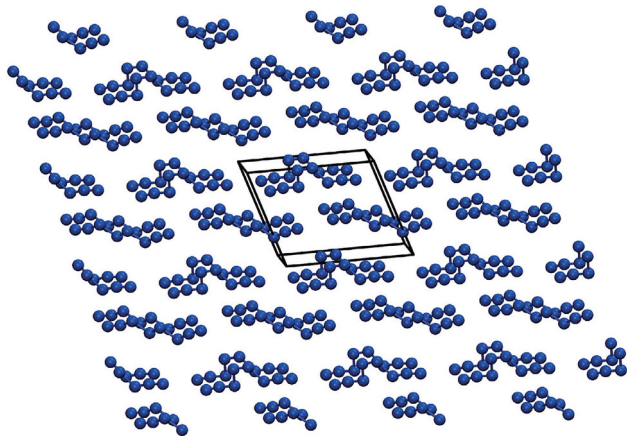

Fig. 4. Crystal structure of $N_8$ solid showing unit cell detailed in Fig. 3.

## EXPERIMENTAL METHODS

Short multiwall carbon nanotubes were obtained from Cheap Tubes Inc. (Brattleboro, VT). The as-received nanotubes used were about 400–600 nm in length and were intentionally chosen to be short in length for our synthesis to allow for the nitrogen oligomer to form inside the tubes. The carbon nanotube powder was mixed with sodium dodecyl sulfate (SDS) surfactant followed by horn sonication and a vacuum filtration process to produce free-standing nanopaper substrates. The nanopaper that formed was then dipped in sodium azide in a pH 4 aqueous buffer solution overnight and then dried in air for a few hours.

The schematic of the plasma apparatus used for the synthesis is depicted in Fig. 6. Nitrogen or ammonia and argon or hydrogen were fed into the quartz tube through needle valve flow meters allowing control of the flow rate of the gas precursors. An adjustable radio frequency generator delivering up to 500 W was attached to an adjustable impedance matching box. The real plasma power was thus the difference between the incident power from the generator and the reflected power. This provided flexibility to choose from a large range of powers. Tuning this power to between 65 W and 70 W was crucial for getting the best synthesis/deposition possible. Throughout this

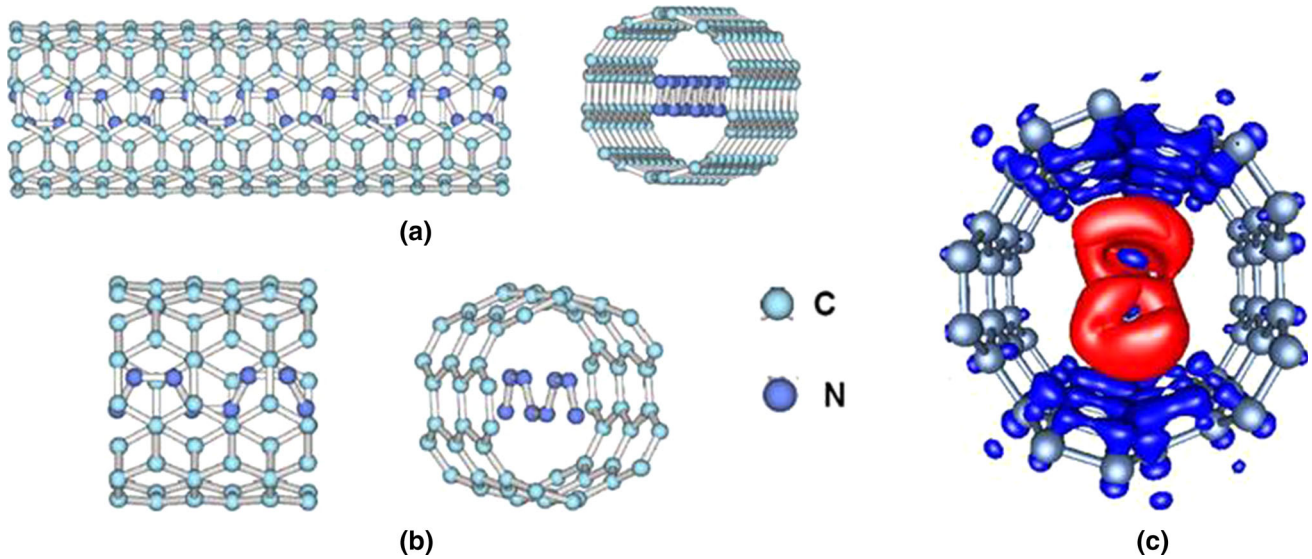


Fig. 5. Nitrogen clusters stabilized inside single walled carbon nanotubes: (a) $N_{24}$ in (5; 5) CNT with nine unit cells. (b) $N_8$ In (5, 5) CNT with three unit cells. (c) Electronic density of $N_8$ in (5; 5) CNT with three unit cells.[9]

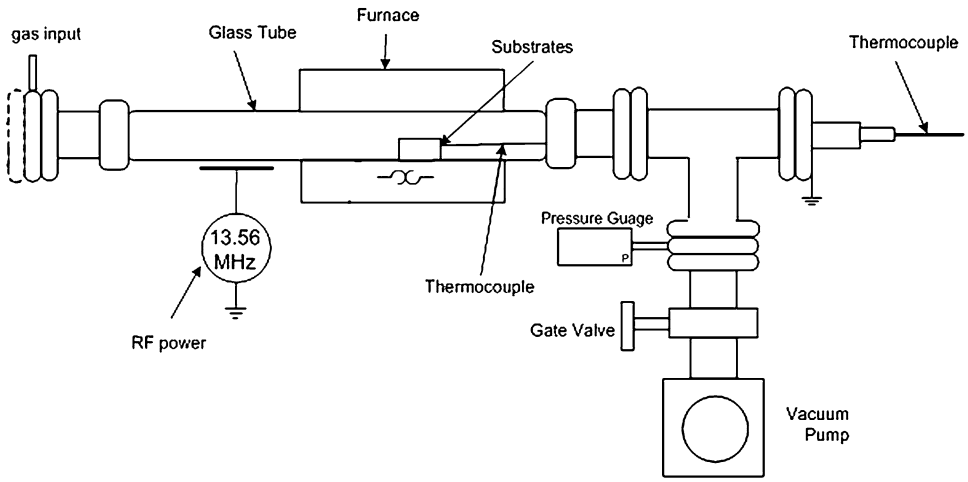


Fig. 6. Schematic of the plasma system reactor used in this study.

study, a power of 65 W was maintained. Gas mixtures of 50% nitrogen and 50% argon were introduced into the deposition chamber where a quartz boat was used to hold a 2 cm × 2 cm nanopaper substrate. A vacuum pump was used to evacuate the deposition chamber to pressures below 1 Torr. When pressures above 1 Torr were used, there was no evidence of PN formation. Flow rates of 15 sccm (standard cubic centimeters per minute) were maintained for each gas. Optimal PN synthesis on the nanopaper substrates was not obtained at higher flow rates. The deposition time was typically between 2 h and 3 h, and at least 2 h was required for optimal synthesis. The temperature of the substrate throughout each experiment was monitored using a thermocouple even though external heat was not applied to the reactor. A temperature of 200°C at 65 W was obtained by intrinsic plasma heating and had to be maintained below 300°C to avoid extensive sodium azide decomposition during the plasma synthesis/deposition process.

Fourier transform infrared (FTIR) spectroscopy was conducted using a Magna Model 560 instrument (Nicolet Instrument Corporation, Madison, WI, USA) attached to an attenuated total reflectance (ATR) accessory with a single reflection ZnSe crystal (MIRacle; Pike Technologies, Madison, WI, USA). The reacted and pristine carbon nanotube nanopaper samples were directly sampled in a range from 600 $cm^{-1}$ to 4000 $cm^{-1}$ at a spectral resolution of 4 $cm^{-1}$. Raman spectroscopy was carried out with a MicroRaman model Thermo Scientific DXR spectrometer (Thermo Scientific, Waltham, MA, USA) with 532-nm laser excitation at a spectral resolution of 2 $cm^{-1}$ and a spatial resolution of 10 $\mu$m. Scanning electron microscope (SEM) images were obtained with a VP-1530 Carl

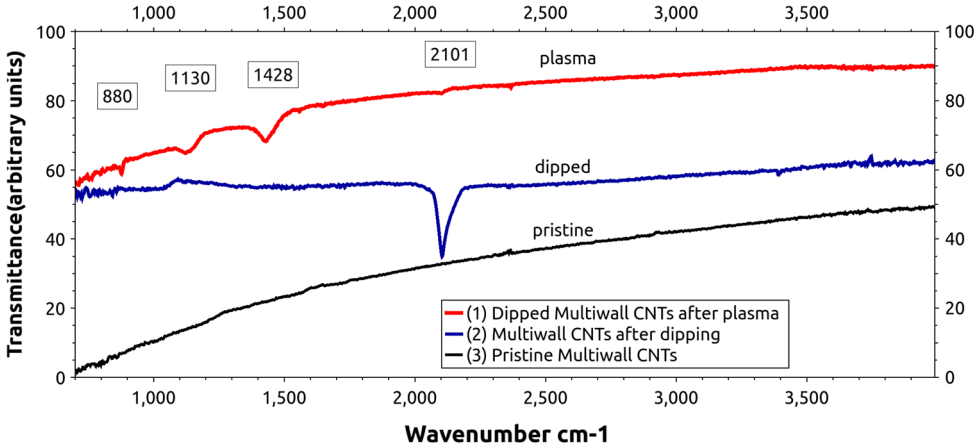


Fig. 7. FTIR spectra of pristine multiwall CNTs, sodium-azide-dipped CNTs, and plasma synthesized PN from sodium-azide-dipped CNT nanopaper samples.

Zeiss LEO (Carl Zeiss, Peabody, MA, USA) field-emission SEM. The samples were mounted on aluminum stubs using double-sided carbon tape. Transmission electron microscope (TEM) images were obtained with a FEI CM-20 Field Emission Gun (FEG) (S)TEM (FEI Company, Hillsboro, OR, USA) equipped with an Enfina PEELS spectrometer (Gatan, Pleasanton, CA, USA) and an Oxford Max-80 Silicon Drift Detector (SDD) Energy Dispersive Spectroscopy (EDS) system (Oxford Instruments, Oxfordshire, UK). The samples were suspended in ultrapure methanol at 1 wt.% concentration, and a 1-$\mu$L drop of the solution was placed on a lacey carbon grid sitting on a filter paper. The TEM grid was then placed in a vacuum oven to dry at 80°C.

## RESULTS AND DISCUSSION

For the related synthesis of diamond by plasma techniques, carbon precursors, such as methane and hydrogen, are usually introduced into the deposition chamber to allow diamond growth on a silicon substrate at temperatures above 800°C. In the current work, carbon nanotubes provided the ideal substrate for the reasons discussed above, whereas azide nuclei from sodium azide, and gases such as nitrogen, ammonia, and hydrogen in argon provided the precursors for PN synthesis. The building block toward $N_5^+$ synthesis[2] was to get $N_5^+$ by letting hydrozoic acid $HN_3$ react with a $N_2F^+$ salt. A mechanism that starts the polymerization can be as follows:

$$\left[|\underline{\bar{N}} - N \equiv N|\right]^- + N^+ \rightarrow [\langle N = N = N = N\rangle]^0 \quad (2)$$

$$[\langle N = N = N = N\rangle]^0 + N^+ \rightarrow [\langle N = N = N = N = N\rangle]^+. \quad (3)$$

Ionized atoms or molecules from molecular nitrogen or ammonia can involve $N_2^+$, $N^+$, $N_2^-$ and $N^-$. The polymerization, driven by structural and electronic stability, can go beyond $N_5^+$ as follows:

$$[\langle N = N = N = N = N\rangle]^+ + N^- \rightarrow [\langle N = N = N = N = N = N\rangle]^0 \quad (4)$$

$$[\langle N = N = N = N = N = N\rangle]^0 + N^+ \rightarrow [\langle N = N = N = N = N = N = N\rangle]^+. \quad (5)$$

Polymerization to PN can take place by alternating between different nitrogen species as needed to transition to a more favorable structure by feeding ionized nitrogen from the plasma jet. The nonequilibrium environment of the plasma facilitates quenching to occur on the surfaces and the insides of the carbon nanotubes. The mechanism does not have to start with the azide anion but can also initiate with $N_2^+$ and $N_2^-$ changing to $N_4$ and then proceeding to larger oligomers. Linear chains of nitrogen clusters or oligomers were considered because of the observation of lines above 2000 $cm^{-1}$ in the FTIR and Raman spectra, which is unlikely for most closed or benzene-like structures.

The FTIR spectrum of the multiwall carbon nanopaper, before and after synthesis, is shown in Fig. 7. The strongest line, at 1,428 $cm^{-1}$, is the sharpest feature. The most recent study on the promising $N_8$ molecular solid reports frequencies in this range (1490.60 $cm^{-1}$ for the EZE conformational isomer shown in Fig. 3 and 1430.69 $cm^{-1}$, 1482.59 $cm^{-1}$ for the solid).[8] A very narrow peak at 880 $cm^{-1}$ was always observed in the FTIR spectra. At first, it was suspected to be an artifact because of its small linewidth, but it is reproducible after each plasma synthesis suggesting that it is related to PN. A peak, at 1130 $cm^{-1}$, is also clear from the spectrum.

Figure 8 shows the Raman spectra of the pristine multiwall carbon nanotubes, the $NaN_3$-dipped

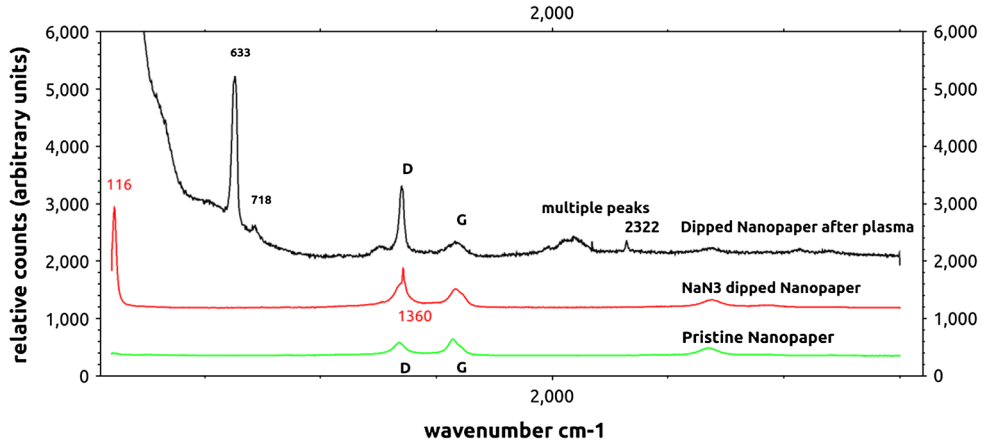


Fig. 8. Raman spectra of the (a) pristine multiwall CNTs, $NaN_3$-dipped CNTs, and plasma synthesized of the $NaN_3$-dipped CNTs.

nanopaper, and the plasma-reacted nanopaper. The D and G bands of the pristine nanopaper are located at 1343 $cm^{-1}$ and 1576 $cm^{-1}$, respectively, with a ratio of $I_d/I_g$ = 0.90. The D and G frequencies shifted slightly in the dipped sample to 1348 $cm^{-1}$ and 1586 $cm^{-1}$, respectively, and their ratio changed by a small amount to 1.06. However, after the plasma synthesis, the nanopapers exhibited a dramatic change. Although the D and G bands did not exhibit a noticeable shift in frequency relative to the dipped sample (D at 1350 $cm^{-1}$ and G at 1586 $cm^{-1}$), the increase of the D mode intensity was huge, rising to a $I_d/I_g$ ratio of 1.40. This can be clearly attributed to substantial creation of defects on the nanotube sidewalls due to the plasma reactions occurring to form PN oligomers. The sharp lines, at 116 $cm^{-1}$ and 1360 $cm^{-1}$, can be assigned to the librational lattice mode and symmetric stretching vibration of the linear azide ion, respectively, from remnants of sodium azide on the substrate. The most remarkable feature in our plasma-synthesized sample, however, is the appearance of a new strong line at 633 $cm^{-1}$. We also detect a line at 718 $cm^{-1}$, a broad bump in the 2000 $cm^{-1}$ region, with peaks at the following wavenumbers ($cm^{-1}$): 1985, 2050, 2095, and 2172, and a sharp peak at 2322 $cm^{-1}$.

The appearance of the line at 633 $cm^{-1}$ was crucial as it provides strong evidence for the N-N single bond in a PN structure. The vibrational peak at 840 $cm^{-1}$ for the single-bonded cubic gauche structure, prepared under high pressure, is predicted to extrapolate to the vicinity of 600 $cm^{-1}$ near ambient pressure.[3] More evidence of this frequency was reported in other studies.[10] The peaks in the vicinity of 2000 $cm^{-1}$ can be attributed to the double-bonded N=N vibrations of the PN structure produced, whereas the highly reproducible sharp peak at 2322 $cm^{-1}$ can be assigned to a triply bonded nitrogen–nitrogen vibration probably from molecular $N_2$ trapped within the nanotube walls or in the PN structure during the plasma reaction.

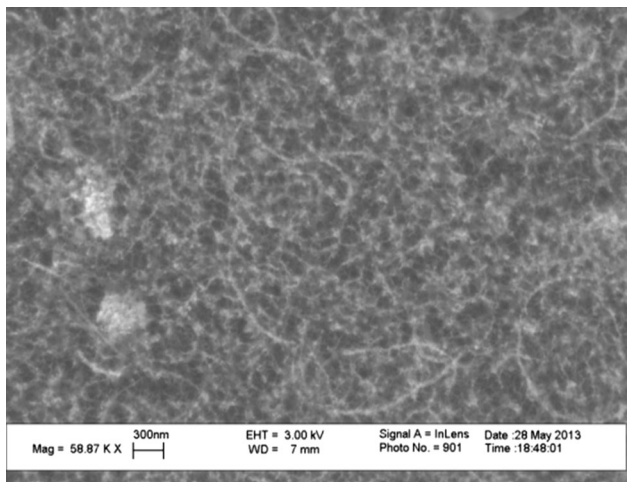


Fig. 9. SEM micrographs of the pristine multiwall CNTs.

The SEM micrographs of the pristine nanopaper, before and after plasma synthesis, along with energy-dispersive x-ray (EDX) analysis are shown in Figs. 9 and 10, respectively. The fibrous features of multiwall carbon nanotubes are clearly seen from the pristine nanopaper. The plasma-reacted sample, on the other hand, looks cloudy and coated, and somehow more stretched. Although no damage appears to have taken place, this cloudy, coated appearance reinforces our belief that the chain-like PN structures form first on the outside surfaces and then inside the nanotubes. High-resolution TEM is planned to confirm this hypothesis. The dramatic increase in the defect D-mode Raman intensity provides strong support for this assumption as pointed out above. This dramatic increase in D-mode intensity is not observed in samples that were just dipped in sodium azide solution.

EDX analysis (Fig. 11) was carried out to gain some quantitative insight about the elements present in the sample. Quantities of up to 17% of nitrogen were detected, part of which probably

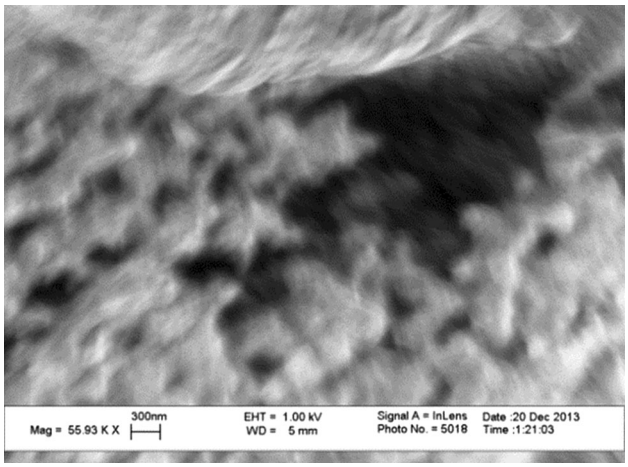


Fig. 10. SEM micrographs of the sodium-azide-dipped multiwall CNTs after plasma reaction.

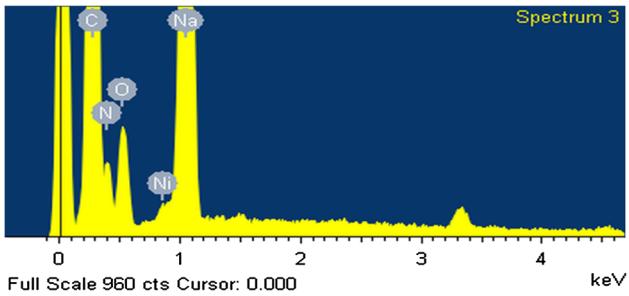


Fig. 11. Elemental EDX analysis of a plasma-synthesized PN sample.

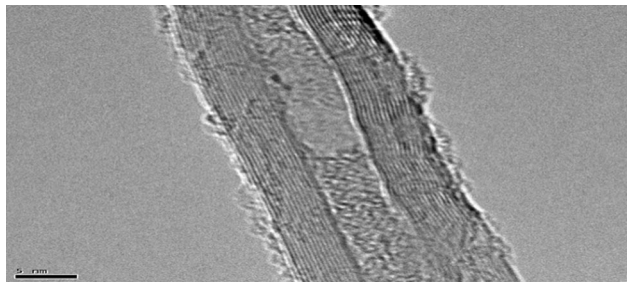

Fig. 12. High-resolution TEM image of a PN/multiwall carbon nanotubes sample deposited under relatively low-RF plasma power of 65 W.

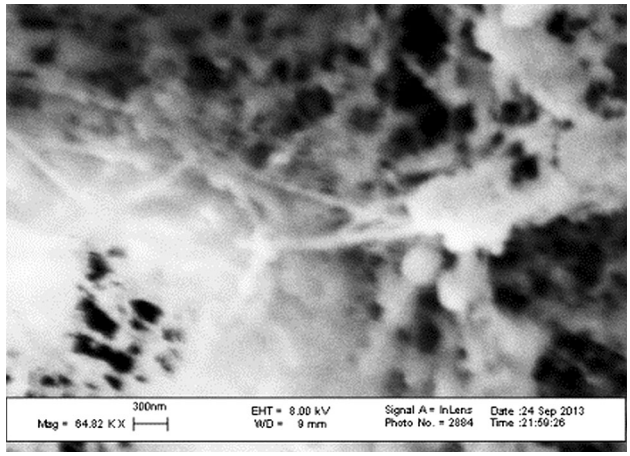


Fig. 13. SEM image of a PN/multiwall carbon nanotubes sample prepared under the same conditions.

comes from remnants of sodium azide in the samples detected in the Raman spectra. Besides carbon and sodium, oxygen from the air present in the plasma reactor and nickel from the catalyst used in carbon nanotube synthesis, were detected.

## Plasma Synthesis of PN Without Azide Precursors

As mentioned earlier, tuning the plasma to the right conditions to synthesize the polymeric nitrogen clusters does not specifically require precursor nuclei like the azides. Gaseous ammonia or nitrogen in argon or hydrogen can be used to synthesize PN on nanopaper substrates, but the amounts produced have been typically small. The goal to synthesize PN without relying on azides is of great importance; therefore, we plan to optimize a more environmentally friendly approach beyond the hazards of a chemical compound like sodium azide. Figure 12 shows a high-resolution TEM of the sample prepared using nitrogen as the precursor. The TEM micrograph shows that the inside of the carbon nanotube is filled with a possibly nitrogen material based on electron energy loss spectroscopy. Although a reliable selected-area electron diffraction could not be obtained, it is likely that the solid structure formed is amorphous. However, in the light of the most recent report of the $N_8$ linear chains coming together to form a highly ordered molecular crystal as a more energetically favorable configuration, and with the knowledge gathered working with the azide ion as the starting material to start the polymerization process, $N_8$-like linear chains are the best candidates to be the building blocks of a PN structure. Figure 13 is an SEM image of a sample synthesized under similar conditions. It reveals that the morphology of the carbon nanotubes is more stretched and coated. Some spherical-shaped structures, about 200 nm in diameter, can be seen connecting the nanotubes similar to that seen in azide prepared samples in Fig. 10.

## Density Functional Calculations

The most challenging feature of working with PN precursor compounds and ions is that only $N_2$, $N_3^-$, $N_4^+$, $N_5^+$, and the high-pressure/high-temperature cubic gauche have been synthesized or ephemerally detected. Spectroscopic data are thus nonexistent for any novel polymeric nitrogen that might be formed. Significant theoretical efforts were therefore made to narrow down the most likely configurations that might appear to help experimentalists

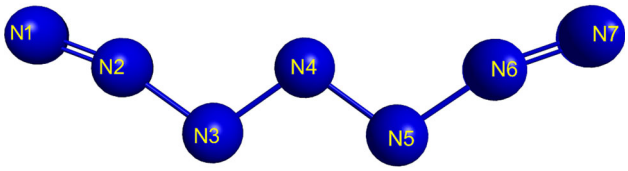


Fig. 14. $N_7^+$ optimized structure.

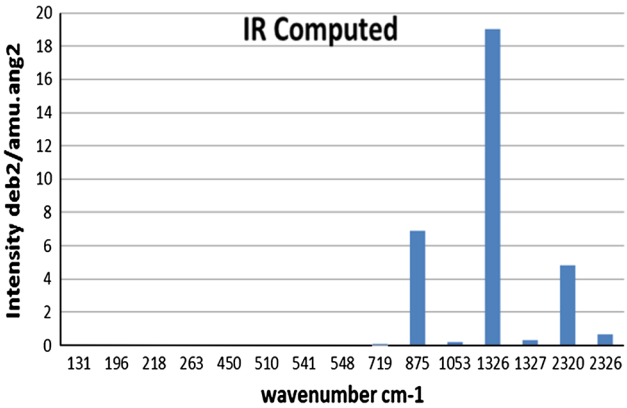


Fig. 15. $N_7^+$computed IR spectrum.

identify them. Clusters from $N_4$, $N_6$, $N_7$, $N_8$, $N_{14}$, $N_{24}$, and up to larger clusters like $N_{60}$ have been studied and proven to be stable.[11–14] To identify the PN synthesized in this work, some geometrical configurations were ruled out and only linear chains without cross-linking were considered. The choice was not arbitrary. But, as mentioned, the search for the best candidate was based on our experimental observations, especially with Raman and FTIR spectroscopy, and many synthesized samples where it was observed. Here, structures and IR/Raman vibrational frequencies for the linear chains of $N_7^+$ and $N_9^+$are reported. The two structures showed no negative frequencies, indicating that a minimum on the potential energy surface was achieved. The interesting feature is the geometrical resemblance with the already successfully synthesized $N_5^+$ and the recently predicted $N_8$ linear chain. Structures like these are promising as they tend to be stable in the gas phase, a preliminary requirement toward stability in a crystalline form without interaction with neighboring sites[8] or in a matrix like carbon nanotubes on which the current approach is based. Our calculations were carried out by density functional theory at the 6-31+G (d, p) level using GamessUS,[15,16] and the structures were visualized with MacMolPlot,[17] a graphical interface to GamessUS. We chose to adopt the B3LYP functional with the 6-31+G (d, p) as it yields the closest results for the well-known azide ion. Wave numbers are expressed in $cm^{-1}$, IR intensities in $debye^2/amu.ang^2$, whereas Raman intensities are expressed in $ang^4/amu$. The azide anion structure optimization, in this study, was for the sole purpose

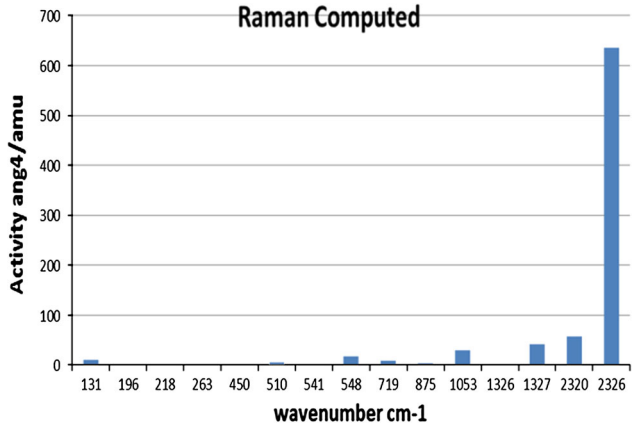


Fig. 16. $N_7^+$ computed Raman spectrum.

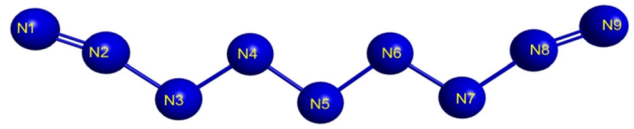


Fig. 17. $N_9^+$ optimized structure.

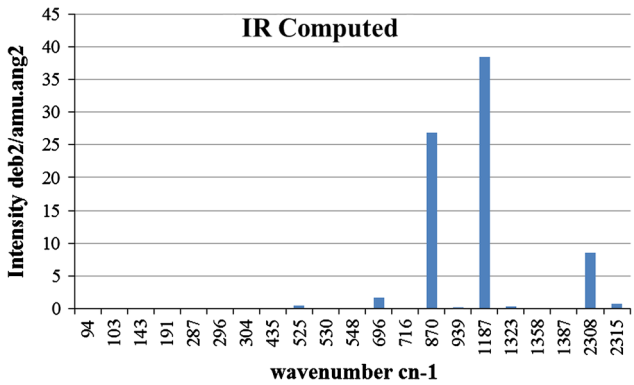


Fig. 18. $N_9^+$ computed IR spectrum.

of testing the validity of our method. There is a deviation of 2.9% for the main IR antisymmetric stretching frequency at 2160 $cm^{-1}$, which was observed experimentally at 2100 $cm^{-1}$, while we recorded a deviation of only 0.29% for the symmetric stretching Raman frequency at 1,364 $cm^{-1}$, which was observed experimentally at 1360 $cm^{-1}$. The results are shown below in Figs. 14, 15, 16 showing the $N_7^+$ ion linear chain and in Figs. 17, 18, 19 showing the $N_9^+$ ion linear chain.

## CONCLUSION

In conclusion, the synthesis of polymeric nitrogen clusters by radio frequency plasma-enhanced chemical vapor deposition has been shown to be clearly feasible using azide ions as precursors and will provide a facile, scalable, and near-ambient conditions alternative to the high-pressure/high-temperature

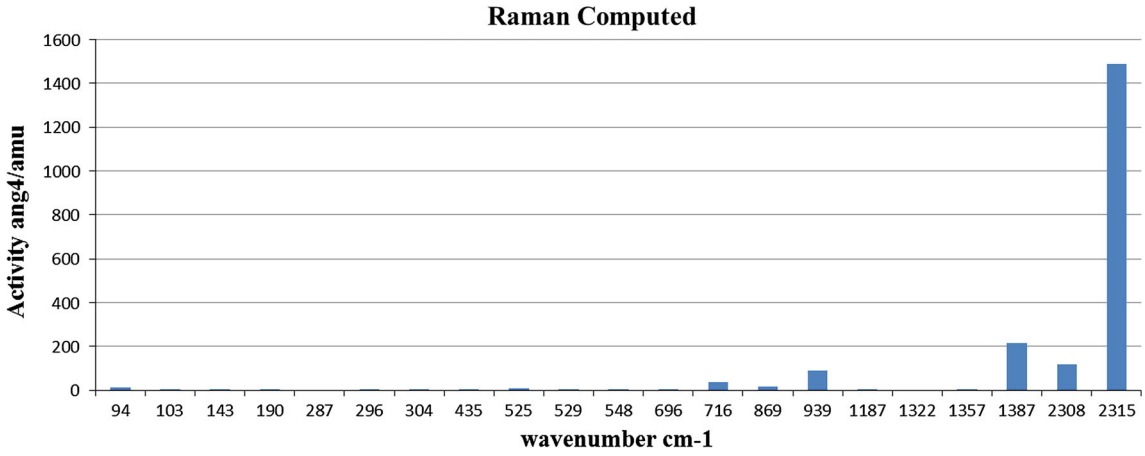


Fig. 19. $N_5^+$ computed Raman spectrum.

approaches. The vibrational frequencies obtained experimentally from our synthesis still do not match the chain-like structures suggested, but they cannot be ruled out because the predictions are for free-standing entities in the gas phase, an essential requirement for the overall stability in any matrix. Our investigation is ongoing about the precise role of the carbon nanotube substrates. The carbon nanotube matrix will definitely shift the frequencies along with their intensities. An example is provided in the most recent work with the $N_8$ molecular structure for which first new frequencies had to emerge that take the whole lattice into consideration and second a frequency shift of the free-standing monomer must occur when embedded in the molecular structure. The structures suggested have no negative frequencies indicating their metastability. A common feature among them is the double bonds at both ends of the molecules giving rise to symmetric and antisymmetric stretch IR and Raman activity. What we see in our Raman spectra after synthesis is a bump made out of many peaks, and we believe that the carbon nanotube matrix must be responsible for both the shift and the decrease in intensity of these two important normal modes of all the structures presented.

## ACKNOWLEDGEMENTS

The authors thank ARDEC, Picatinny Arsenal, New Jersey Institute of Technology, CarboMet LLC for support; and Drs. Rajen Patel (ARDEC) and Alex Chou (Stevens Institute of Technology) for the TEM characterization. The work was supported in part by an NSF CBET 1231682 grant and thanks are due to Professor Xianqin Wang for extensive discussions.

## REFERENCES

1. K.O. Christe, *Propellant Explos. Pyrotech.* 32, 194 (2007).
2. K.O. Christe, W.W. Wilson, J.A. Sheehy, and J.A. Boatz, *Angew. Chem. Int. Ed.* 38, 2004 (1999).
3. M.I. Eremets, A.G. Gavriliuk, I.A. Trojan, D.A. Dzivenko, and R. Boehler, *Nat. Mater.* 3, 558 (2004).
4. T.W. Barbee, *Phys. Rev. B* 48, 9327 (1993).
5. M.I. Eremets, R.J. Hemley, H.-K. Mao, and E. Gregoryanz, *Nature* 411, 170 (2001).
6. F. Zahariev, J. Hooper, S. Alavi, F. Zhang, and T.K. Woo, *Phys. Rev. B* 75, 140101 (2007).
7. S. Fau and R.J. Bartlett, *J. Phys. Chem. A* 105, 4096 (2001).
8. B. Hirshberg, R.B. Gerber, and A.I. Krylov, *Nat. Chem.* 6, 52 (2014).
9. H. Abou-Rachid, A. Hu, V. Timoshevskii, Y. Song, and L.-S. Lussier, *Phys. Rev. Lett.* 100, 196401 (2008).
10. J.A. Ciezak and J.A. Timothy, *Metastable Polymeric Nitrogen From N2H2 Alloys* (2008), http://handle.dtic.mil/100.2/ADA505734.
11. J. Guan, S. Zhang, W. Xu, and Q. Li, *Struct. Chem.* 15, 121 (2004).
12. T.-K. Ha and M.T. Nguyen, *Chem. Phys. Lett.* 195, 179 (1992).
13. T.-K. Ha, O. Suleimenov, and M.T. Nguyen, *Chem. Phys. Lett.* 315, 327 (1999).
14. P.C. Samartzis and A.M. Wodtke, *Int. Rev. Phys. Chem.* 25, 527 (2006).
15. M.S. Gordon and M.W. Schmidt, *Theory and Applications of Computational Chemistry*, ed. C.E. Dykstra, G. Frenking, K.S. Kim, and G.E. Scuseria (Amsterdam, The Netherlands: Elsevier, 2005), pp. 1167–1189.
16. M.W. Schmidt, K.K. Baldridge, J.A. Boatz, S.T. Elbert, M.S. Gordon, J.H. Jensen, S. Koseki, N. Matsunaga, K.A. Nguyen, S. Su, T.L. Windus, M. Dupuis, and J.A. Montgomery, *J. Comput. Chem.* 14, 1347 (1993).
17. B.M. Bode and M.S. Gordon, *J. Mol. Graph. Model.* 16, 133 (1998).